Thermoelectric Properties of Mg_{2}(Ge,Sn): Model and Optimization of ZT

Jifeng Sun and David J. Singh

Phys. Rev. Applied **5**, 024006 — Published 16 February 2016

DOI: 10.1103/PhysRevApplied.5.024006

Thermoelectric properties of Mg_2(Ge,Sn): Model and optimization of ZT

Jifeng Sun and David J. Singh*
Department of Physics and Astronomy, University of Missouri-Columbia, Columbia, MO 65211, USA
(Dated: January 29, 2016)

We report an investigation of the thermoelectric properties of $Mg_2Ge_{1-x}Sn_x$ solid solution with $x = 0.5$ using models based on first-principles calculations and experimental data. The model gives transport properties including the figure of merit ZT as functions of carrier concentration and temperature. The model for n-type predicts high ZT at optimized doping, and suggests that the ZT value can exceed 2 at $T = 1000$ K.

I. INTRODUCTION

Themoelectric (TE) materials are of interest due to applications in power generation and refrigeration. Applications such as waste heat recovery, e.g., in automobiles, will require practical materials that are both amenable to manufacturing and have high performance in the 500 K - 1000 K temperature range[1–3]. The performance of a TE material is characterized by a dimensionless figure of merit $ZT = \sigma S^2 T/(\kappa_l + \kappa_e)$, and σ, S, T, κ_l and κ_e are electrical conductivity, Seebeck coefficient, temperature, lattice and electronic contributions to the thermal conductivity, respectively. Much effort has been focused on improving and optimizing ZT by increasing the power factor $S^2\sigma$ or reducing the thermal conductivity[4–6]. State-of-the-art TE materials such as the commercialized $(Bi,Sb)_2Te_3$ derived alloys[7,8], PbTe and related alloys[9–11], some skutterudite alloys[12,13] have $ZT > 1.0$ in a intermediate operating temperature range (500 K $\sim$ 1000 K). For applications, practical materials that have environmentally acceptable composition are important.

The solid solutions of Mg_2X (X = Si, Ge and Sn) are promising candidates for mid-temperature range energy conversion[14–31]. Most of the work has been focused on the Mg_2Si-Mg_2Sn alloys. The ZT of n-type compositions are significantly higher than those of p-type. In particular, the ZT values of n-type $Mg_2Si_{0.5}Sn_{0.5}$ systems can reach 1.5[24] at 600 K by varying x value. Recently, Liu and co-workers[29] have successfully synthesised $Mg_2Sn_{0.75}Ge_{0.25}$ that with n-type ZT value of 1.4 at 450 °C. Comparing to n-type, the reported p-type Mg_2X solid solutions have much lower ZT values, with about 0.35 for Mg_2Si-Mg_2Sn alloy[32], 0.36 for Mg_2Si-Mg_2Ge alloy[19] and up to 0.38 for Mg_2Ge-Mg_2Sn[28].

Here we address the thermoelectric properties of Mg_2Ge-Mg_2Sn solid solution, with a typical composition of $Mg_2Ge_{0.5}Sn_{0.5}$, from a combination of first-principles calculations and analysis of existing experimental data. By optimizing the ZT with respect to the doping concentrations at different temperatures, we find a peak ZT value of 2.25 for n-type and 0.4 for p-type at 1000 K and reasonable high doping concentrations ($\sim 10^{20}$ cm^{-3}). Thus the material can be further improved by tuning the carrier concentrations.

II. COMPUTATIONAL APPROACH

The semiquantitative models for both n- and p-type $Mg_2Ge_{0.5}Sn_{0.5}$ are based on existing experimental data and first-principles calculations. Specifically, due to the lack of the data on $Mg_2Ge_{0.5}Sn_{0.5}$, we used data for $Mg_2Ge_{0.4}Sn_{0.6}$ to model our p-type ZT and $Mg_2Ge_{0.25}Sn_{0.75}$ for n-type case. The construction of the model is similar to a model previously made for PbSe[33], which predicted that ZT could significantly exceed the known values, a fact that was later confirmed experimentally[34]. We also investigated a higher Sn composition, $Mg_2Ge_{0.25}Sn_{0.75}$ in order to study the effects of composition dependent band structure change. The theoretical transport functions and coefficients were obtained using Boltzmann theory within the constant scattering time approximation (CSTA) as implemented in the BoltzTraP code[35]. This CSTA approach has been successfully applied in calculating the Seebeck coefficient for various TE materials[36–39]. It assumes the energy dependence of the scattering rate is negligible compared with the energy dependence of the electronic structure.

The band structure calculations were performed using the linearized augmented plane-wave (LAPW) method[40] as implemented in the WIEN2K code[41]. The crystal structure of $Mg_2Ge_{0.5}Sn_{0.5}$ solid solution was modeled by doubling the original cubic structure to a $P4/mmm$ tetragonal structure (formula, Mg_4GeSn) with Ge at (0,0,0), Sn at (1/2,1/2,1/2) and Mg at (0,1/2,z), as shown in Fig. 1. The experimental lattice constants of $Mg_2Ge_{0.5}Sn_{0.5}$[28] were used and the atomic coordinates were relaxed within the Perdew, Burke and Ernzerhof (PBE) type functional of the generalized gradient approximation (GGA)[42]. We also did calculations for other supercells. This included a larger 24-atom cell with lower symmetry. However we did not find significant changes. The LAPW sphere radii were 2.5 bohr for Mg, Ge and Sn and the cut-off parameter for the basis was $R_{min}K_{max} = 8$. We used a k-point sampling of 5×5×3 for the total energy calculations and a k-mesh of 14×14×10 for the density of states. A much denser k-mesh of 30×30×21 was used for the calculations of isosurfaces and transport properties. The modified Becke-Johnson (mBJ) potential[43] was used to obtain the electronic structures. This potential has been proved to be reasonable for the calculations of semiconductor and in-

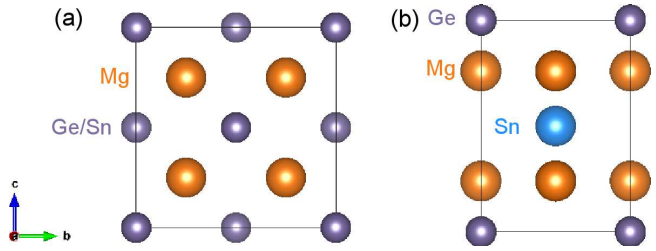

FIG. 1. Crystal structures of $Mg_2Ge_{1-x}Sn_x$ (a) and doubled cell (b) with formula Mg_4GeSn. Solid line indicates the unit cell.

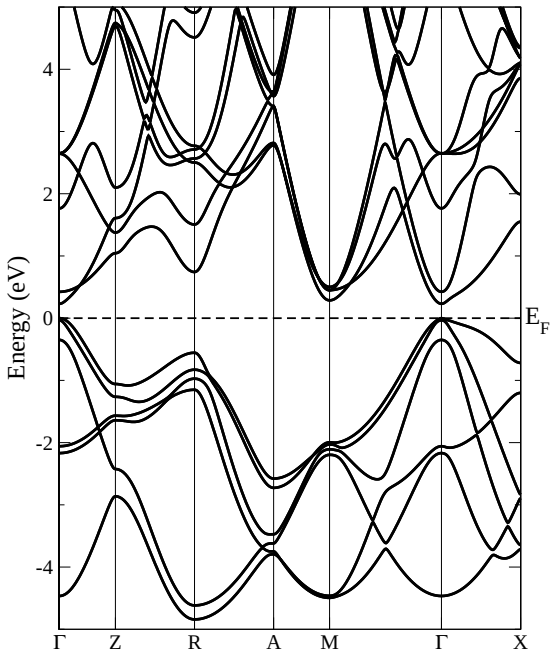

FIG. 2. Calculated band structure of $Mg_2Ge_{0.5}Sn_{0.5}$. Energy zero is set at the valence band maximum.

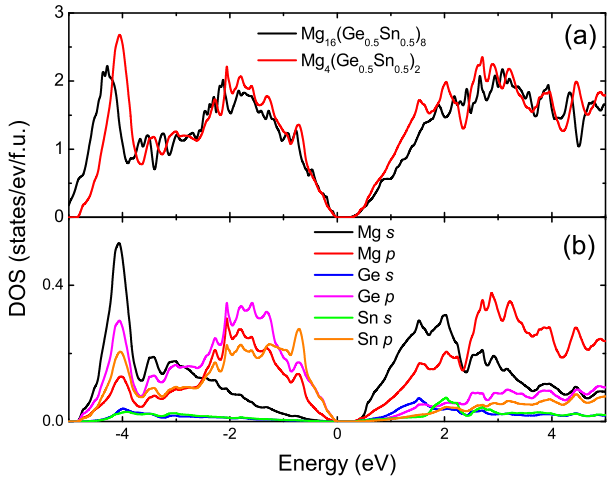

FIG. 3. Total and projected density of states of $Mg_2Ge_{0.5}Sn_{0.5}$ with (a) showing the comparison of two different crystal structures and (b) the projected density of states of the structure used in this study. Density of states are shown per $Mg_2Ge_{0.5}Sn_{0.5}$ formula unit (f.u.).

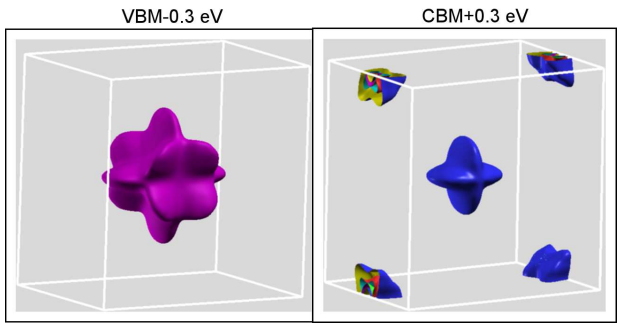

FIG. 4. Calculated isoenergy surfaces of $Mg_2Ge_{0.5}Sn_{0.5}$ near VBM and CBM.

sulator systems and typically gives substantial improved band gaps[43–45]. Spin-orbit coupling was included in all the calculations except structure relaxations.

III. RESULTS AND DISCUSSIONS

The calculated band structure using the mBJ potential is shown in Fig. 2. It has a direct band gap of 0.23 eV at the Γ point. This value is 0.045 eV using PBE functional. The band gap values of pure binary Mg_2Ge and Mg_2Sn were reported to be 0.74 eV and 0.35 eV[46] and our calculated results with mBJ are 0.51 eV and 0.10 eV, respectively. Moreover, it has been demonstrated that the energy gap of $Mg_2Ge_{1-x}Sn_x$ decreases as x increases[28]. Therefore the band gap is improved with the mBJ potential but still underestimate experiment as also seen in Mg_2Si-Mg_2Sn compounds[47]. This may lead to a reduced ZT at high temperature due to overestimating the bipolar contribution, especially for p-type. The composition dependent band convergence is seen in $Mg_2Si_xSn_{1-x}$ alloys[26,48–50]. The nearness of the conduction bands affects the performance, but because kT is e.g. $\sim$ 0.07 eV at 800 K, the multiple nearby bands are important but exact convergence is not so crucial, which reduces composition dependence.

The electronic density of states are presented in Fig. 3. We found similar density of states especially near both the valence band edge and conduction band edge, as shown in Fig. 3 (a) for the different supercells. This supports the use of super cell as chosen and indicates the reliability of our following electronic structure dependent properties calculations. The projected electronic density of states are also depicted in Fig. 3 (b). As seen, the valence band is mainly dominated by anion p states and cation s and p states. A clear overlap between Mg 3s and

Ge $4p$/Sn $5p$ can be seen at -4 eV below the valence band maximum (VBM) indicating the hybridization between Mg and Ge/Sn. The conduction band mainly consists of s and p empty states of Mg. Figure 4 shows the constant energy surfaces at 0.3 eV below and above the VBM and conduction band minimum (CBM), respectively. Both p and n type show complex corrugated isosurfaces, much different from simple spheres. Such complex shapes are generally beneficial for TE performance[51,52]. Moreover, for n-type, in addition to the main surface around Γ, one observes four additional electron surfaces at the zone boundary M point starting close to the gap. These M-point carriers can participate in transport along with the two bands at Γ. Taking Γ and M together the n-type has a high number of pocket available for transport compared to p-type (note that $T = 1000$ K corresponds to $kT \sim 0.1$ eV).

The thermopower plays a central role in the performance of TE materials and can be directly calculated from the electronic structure obtained within the framework of density functional theory. By using of the Wiedemann-Franz relation where the electronic part of the thermal conductivity is expressed as $\kappa_e = L\sigma T$, the figure of merit ZT can be further reconstructed as $ZT = rS^2/L$. Here $r = \kappa_e/(\kappa_e + \kappa_l)$ and $L = 2.45 \times 10^{-8} W\Omega/K^2$ is the standard Lorenz number. The fact that $r \leqslant 1$ implies the upper bound of ZT is limited by the thermopower. For the ZT larger than unity, the thermopower is usually higher than 200 μV/K. The calculated result is shown in Fig. 5. There is a clear bipolar suppression for both p- and n-type at high temperatures and low carrier concentrations. One effect of the bipolar effects seen especially for p-type will be an increase in L, which will lead to higher thermal conductivity and lower ZT. The bipolar effect increases with T but decreases with carrier concentrations. High thermopowers (> 200 μV/K) are obtained even at high temperatures (~ 1000 K) with reasonable carrier concentrations ($\sim 10^{20}$ cm^{-3}) for both n- and p-type. Clearly, optimization of carrier concentration which is crucial for any thermoelectric will be particularly important for any x and operating T in Mg_2(Ge,Sn) due to the bipolar effect.

Within the CSTA, the electrical conductivity is given as $\sigma = (\sigma/\tau) \times \tau$. It is possible to calculate σ/τ directly from electronic structure as a function of carrier concentration and temperature. But one can not solve for σ without the knowledge of τ, which is the inverse of the scattering rate. In a typical electron-phonon regime, τ is proportional to 1/T and decreases with carrier concentration and we take a standard form with $\tau \propto n^{-1/3}$.

In order to model the behavior of τ, the experimental data was used. Specifically for p type $Mg_2Ge_{0.5}Sn_{0.5}$, we used the data from Jiang and co-workers[28] who synthesised the $Mg_2Ge_{0.4}Sn_{0.6}$ solid solution and doped with Ag. We choose the data set at a specific temperature of 400 K. The reported thermopower was about 203 μV/K at this temperature. The corresponding doping level can be obtained by comparing with the calculated $S(T, n/p)$ in Fig. 5 as 4.48×10^{19} cm^{-3}. The reported electrical conductivity was approximately 2.00 $\times10^4$ S/m, which combined with the calculated σ/τ yields $\tau = 1.04 \times 10^{-5} T^{-1} p^{-1/3}$ with τ in s, T in K and p in cm^{-3}. Similarly, we used the same strategy for the n type case. Recently, Liu and co-workers[29] reported a new Mg_2Sn-based n type TE material with formula of $Mg_2Ge_{0.25}Sn_{0.75}$ and the ZT value can be achieved to 1.4 at 450 °C. We conducted the same strategy to produce a second model by using the data at 400 K and the τ was fitted to be $\tau = 7.60 \times 10^{-5} T^{-1} n^{-1/3}$. Note that the corresponding doping level in taking the n type data is calculated to be 5.05×10^{19} cm^{-3}, which is much lower than the measured one (3×10^{20} cm^{-3}). Therefore, we did a comparison calculation by taking the experimental σ and doping concentration. Then we find different $\tau = 3.00 \times 10^{-5} T^{-1} n^{-1/3}$. This other τ ($\tau\prime$) was only used in the model for the final ZT as comparison and our following related results are based on the first τ. As mentioned, the σ can be calculated as $\sigma = (\sigma/\tau) \times \tau$, which is shown in Fig. 6. It is noted that the magnitude of σ is ten times larger for n type compared with p type. But the overall trend is similar in both cases. Similarly, for n type $Mg_2Ge_{0.25}Sn_{0.75}$, we obtained the $\tau = 3.94 \times 10^{-5} T^{-1} n^{-1/3}$.

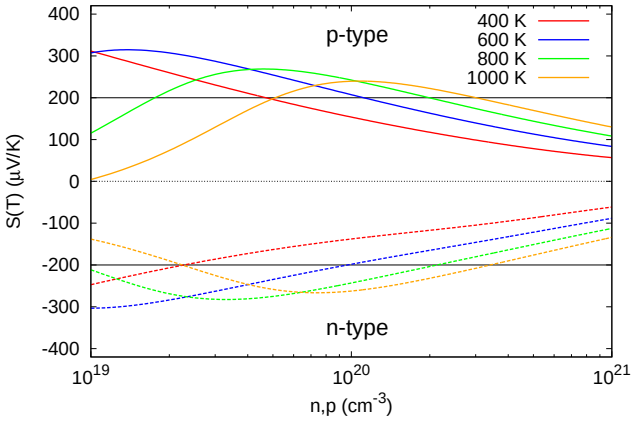

FIG. 5. Calculated $S(T, n/p)$ for both n- and p-type $Mg_2Ge_{0.5}Sn_{0.5}$. Solid horizontal line at 200 μV/K represents the limitation of Seebeck coefficients for good TE materials.

The corresponding power factor is plotted in Fig. 7 for $Mg_2Ge_{0.5}Sn_{0.5}$. For n type, it is seen that the power factor increases with temperature and doping level until reaching the maximum value at 4.5×10^{20} cm^{-3}, with a peak value of 0.012 W/mK^2. This value is about twice the power factor found in Liu's experiment with $Mg_2Ge_{0.25}Sn_{0.75}$ samples and higher but comparable to other calculated results at corresponding temperatures for $Mg_2Si_{1-x}Sn_x$ solid solutions[17,26]. On the other hand, the p type power factor shows weaker T dependent with the peak shifting to higher carrier concentrations with increasing T, e.g., from $p = 4 \times 10^{19}$ cm^{-3} at 400 K to $p = 4 \times 10^{20}$ cm^{-3} at 1000 K with peak value of 0.0015

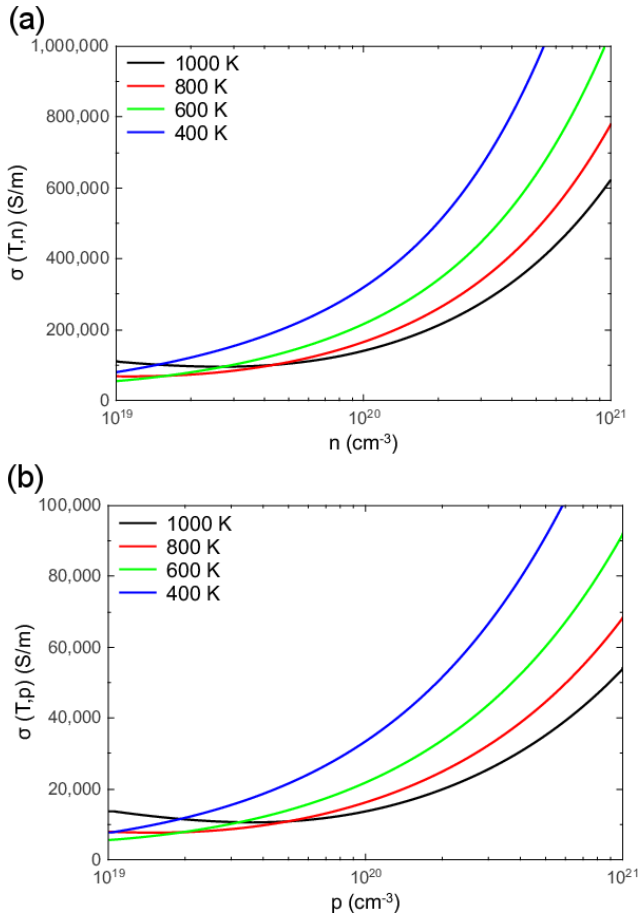

FIG. 6. Calculated electrical conductivity for both n- and p-type $Mg_2Ge_{0.5}Sn_{0.5}$.

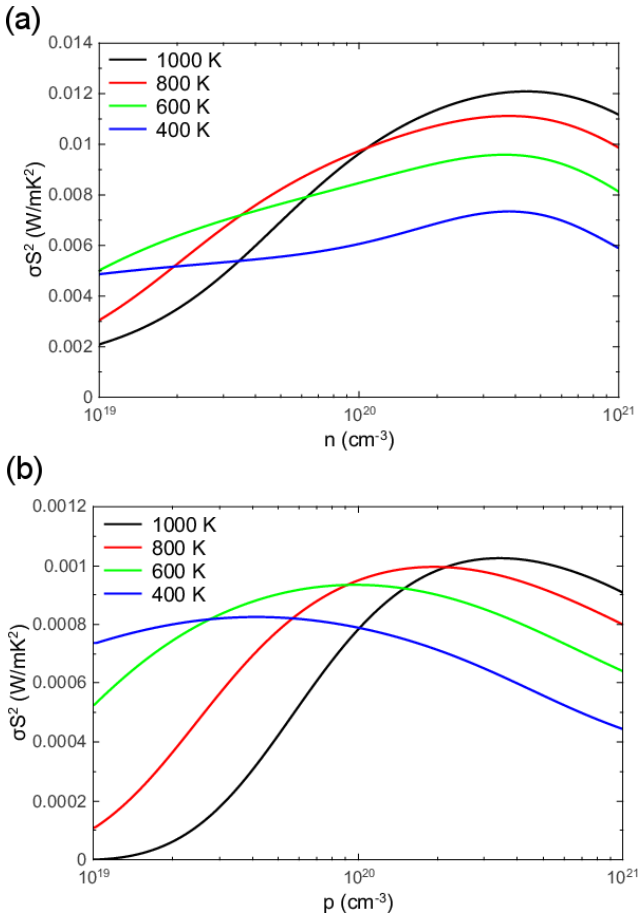

FIG. 7. Calculated power factor for both n- (a) and p-type (b) $Mg_2Ge_{0.5}Sn_{0.5}$.

W/mK^2. The results are in accord with Jiang's data (e.g., 0.0011 W/mK^2 at 650 K for $Mg_2Ge_{0.4}Sn_{0.6}$).

Optimization of ZT also requires the knowledge of the thermal conductivity which consists of the contributions from the lattice and the electronic parts and sometimes including the bipolar effects[24,29]. As mentioned, the electronic part can be directly calculated using the Wiedemann-Franz relation from $\kappa_e = L\sigma T$. The lattice thermal conductivity κ_l typically goes as $1/T$ until high temperatures where it becomes saturated and reaches the limit of thermal conductivity[53]. κ_l is also generally the least dependent on doping. Therefore we can make an estimation of the thermal conductivity as $\kappa = A/T + L\sigma T$. With the calculated σ, the constant A can be determined using the experimental data. Here we chose Jiang's data at low temperature range (300 K - 500 K)for fitting the p-type κ_l. For n type, we adopted the same lattice part for $Mg_2Ge_{0.5}Sn_{0.5}$ but with Liu's data for $Mg_2Ge_{0.25}Sn_{0.75}$. It is noted that the electronic contribution to the total thermal conductivity is substantial at high temperatures in Liu's data and this may lead to larger errors in the extracted lattice thermal conductivity. We use Jiang's data for the model. Using Liu's data leads to a very similar maximum ZT, less than 5% lower. Note that the potential bipolar effects, which are evident at high temperatures and low doping levels are included in the calculations of σ_e. In order to overcome the potential inaccuracy from the strong bipolar effects in the p type case, which is also seen in the experiments[28], the calculated L was used. As shown in Fig. 8, L is clearly a function of doping level and temperature as also observed in analogous compound $Mg_2Si_{1-x}Sn_x$[30]. For n type case, the constant L was used. This is because the p-type mobility is significantly lower than n-type. The results is that bipolar effects are low for n-type, while calculation of L would require assuming equal τ.

In any case, we are able to model ZT as a function of temperature and carrier concentration. Results are given in Figs. 9 and 10 for $Mg_2Ge_{0.5}Sn_{0.5}$ and Fig. 11 for n type $Mg_2Ge_{0.25}Sn_{0.75}$. It is clearly shown that n type material has higher ZT value compared with p type. In particular, the maximum value of ZT increases with increasing doping levels and at elevated temperatures. A peak ZT of 2.25 (2.35 if Liu's data is used for κ_l)for n type $Mg_2Ge_{0.5}Sn_{0.5}$ at 1000 K is found with a doping level of 9×10^{19} cm^{-3}. This ZT value is higher comparing with Liu's experiment (1.4 at 450 °C). Our comparison calculation on n type $Mg_2Ge_{0.25}Sn_{0.75}$ also exhibits high

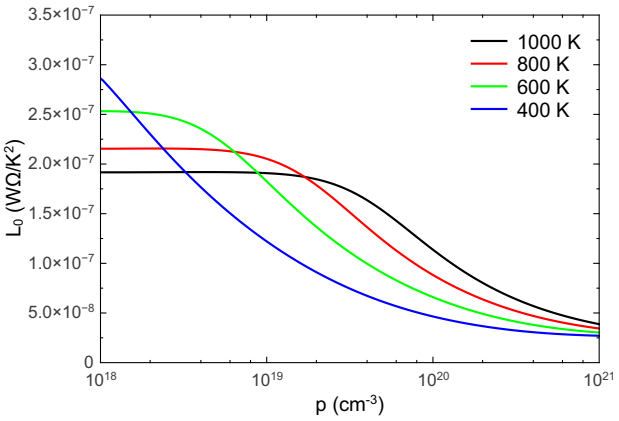

FIG. 8. Calculated L_0 versus temperature and doping concentration for p-type $Mg_2Ge_{0.5}Sn_{0.5}$.

ZT ($\sim$ 2.1), indicating the band structure difference at conduction band edge dos not have significant effects at high T. Figure 12 shows the optimized ZT from the $\tau\prime$ introduced above. As seen the maximum ZT is about 1.7 at 1000 K. This difference might be viewed as an error bar on the model. However it is likely that the $\tau\prime$ result is an underestimate of the ultimate ZT because the temperature dependence of the experimental data upon which it is based suggests the defect scattering is playing a role and could be improved. $Mg_2Ge_{0.5}Sn_{0.5}$ is expected to have larger band gaps with the addition of Ge comparing to $Mg_2Ge_{0.25}Sn_{0.75}$ even $Mg_2Ge_{0.4}Sn_{0.6}$. This suggests the possibility to extend the operating temperature of $Mg_2Ge_{0.5}Sn_{0.5}$ and higher ZT is achievable. On the other hand, the p type material is inferior to n type on the performance with maximum ZT value of 0.4 at 1000 K. Jiang and co-workers[28] reported ZT of 0.38 at 650 K for $Mg_2Ge_{0.4}Sn_{0.6}$ samples, which agree well with our calculated result at corresponding carrier concentration if composition difference is considered. High ZT values up to 1.4 at 900 K was seen in both experiments and theory calculations of n-type Mg_2(Si-Ge-Sn) pseudo-quaternary solid solutions[54,55]. This results from very low thermal conductivity ($\sim$ 2 W/mK) due to multi-phase alloying. This value is lower than Liu's work ($\sim$ 3 W/mK) for $Mg_2Ge_{0.25}Sn_{0.75}$ which can achieve 1.4 ZT at 450 °C.

IV. SUMMARY AND CONCLUSIONS

In summary, we have investigated the electronic and the thermoelectric properties of the Mg_2Ge-Mg_2Sn solid solutions with a typical composition of $Mg_2Ge_{0.5}Sn_{0.5}$. A practical TE device requires both n and p type materials. Thus while the p-type ZT estimated here is not as impressive as n-type the fact that potential improvement can be achieved in $Mg_2Ge_{0.5}Sn_{0.5}$ compared to other Mg_2X solid solutions is important, and suggests

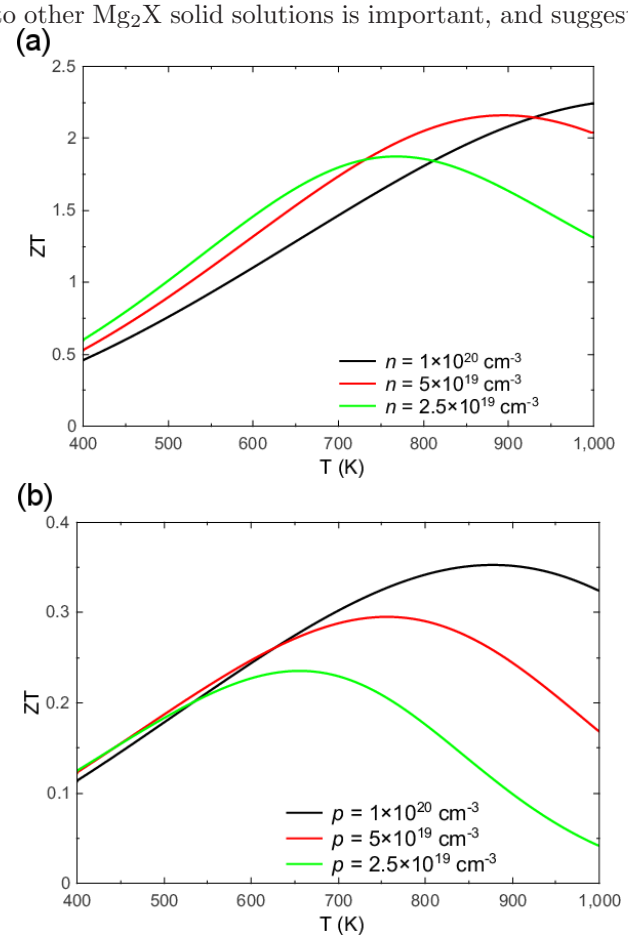

FIG. 9. Calculated ZT versus T for both n- (a) and p-type (b) $Mg_2Ge_{0.5}Sn_{0.5}$ using the model discussed in the text.

efforts to further optimizing the material.

The transport functions and related parameters are calculated using the combination of the existing experimental data and the first principles calculations. We find superior thermoelectric performance in n type material as is known from experimental measurements of Mg_2Ge-Mg_2Sn solid solutions. Importantly, we find high ZT value of 2.25 at 1000 K for n type and 0.4 for p type at the same temperature and similar doping range. In any case, our semiquantitative optimization of ZT with respect to carrier concentrations and temperatures offers a better understanding of this environmental friendly and promising thermoelectric material. The results imply that Mg_2(Ge,Sn) alloys can be further improved through additional optimization of the carrier concentration, and sample quality.

ACKNOWLEDGMENTS

This work was supported by the Department of Energy through the S3TEC Energy Frontier Research Center award # DE-SC0001299/DE-FG02-09ER46577.

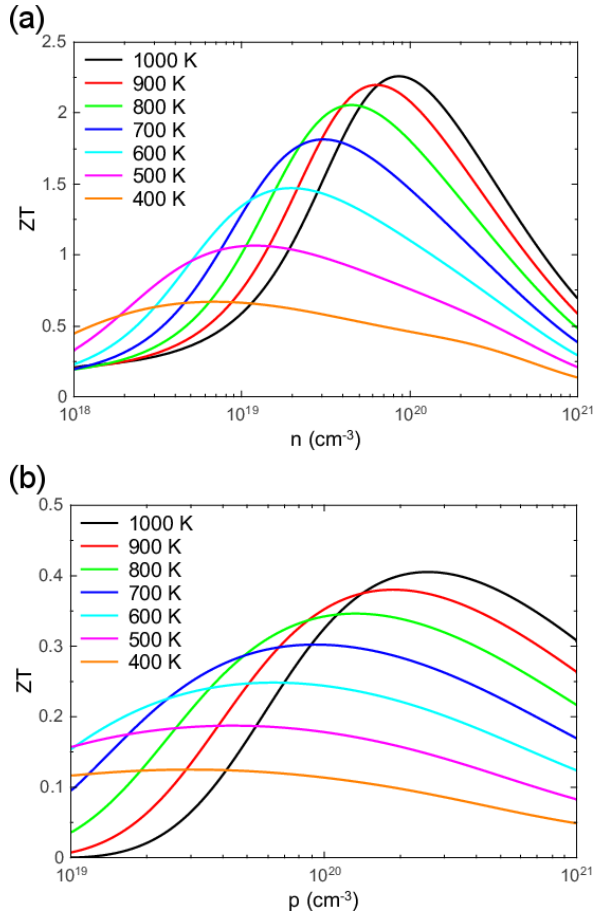

FIG. 10. Calculated ZT versus doping concentration for both n- and p-type $Mg_2Ge_{0.5}Sn_{0.5}$ using the model discussed in the text.

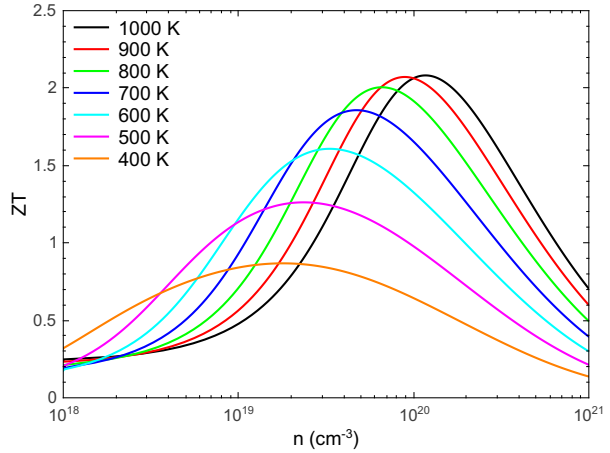

FIG. 11. Calculated ZT versus doping concentration for n type $Mg_2Ge_{0.25}Sn_{0.75}$.

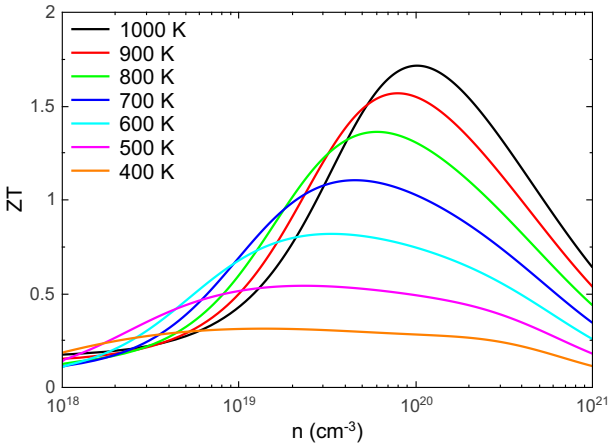

FIG. 12. Calculated ZT versus doping concentration for n type $Mg_2Ge_{0.5}Sn_{0.5}$ using the fitted $\tau\prime$ (see text).

* singhdj@missouri.edu

[1] J. Yang and T. Caillat, "Thermoelectric materials for space and automotive power generation," MRS Bulletin **31**, 224–229 (2006).

[2] J. Yang and F. Stabler, "Automotive applications of thermoelectric materials," J. Electron. Mater. **38**, 1245–1251 (2009).

[3] C. Yu and K. Chau, "Thermoelectric automotive waste heat energy recovery using maximum power point tracking," Energy Conversion and Management **50**, 1506 – 1512 (2009).

[4] J. Sootsman, H. Kong, C. Uher, J. D'Angelo, C.-I. Wu, T. Hogan, T. Caillat, and M. Kanatzidis, "Large enhancements in the thermoelectric power factor of bulk PbTe at high temperature by synergistic nanostructuring," Angewandte Chemie **120**, 8746–8750 (2008).

[5] J.-H. Lee, J. Wu, and J. C. Grossman, "Enhancing the thermoelectric power factor with highly mismatched isoelectronic doping," Phys. Rev. Lett. **104**, 016602 (2010).

[6] W. Kim, J. Zide, A. Gossard, D. Klenov, S. Stemmer, A. Shakouri, and A. Majumdar, "Thermal conductivity reduction and thermoelectric figure of merit increase by embedding nanoparticles in crystalline semiconductors," Phys. Rev. Lett. **96**, 045901 (2006).

[7] O. Yamashita, S. Tomiyoshi, and K. Makita, "Bismuth telluride compounds with high thermoelectric figures of merit," J. Appl. Phys. **93**, 368–374 (2003).

[8] Y. Ma, Q. Hao, B. Poudel, Y. Lan, B. Yu, D. Wang, G. Chen, and Z. Ren, "Enhanced thermoelectric figure-of-merit in p-type nanostructured bismuth antimony tellurium alloys made from elemental chunks," Nano Lett. **8**, 2580–2584 (2008).

[9] K. Biswas, J. He, Q. Zhang, G. Wang, C. Uher, V. P. Dravid, and M. G. Kanatzidis, "Strained endotaxial nanostructures with high thermoelectric figure of merit," Nat. Chem. **3**, 160 – 166 (2010).

[10] J. P. Heremans, V. Jovovic, E. S. Toberer, A. Saramat, K. Kurosaki, A. Charoenphakdee, S. Yamanaka, and G. J. Snyder, "Enhancement of thermoelectric efficiency in PbTe by distortion of the electronic density of states," Science **321**, 554–557 (2008).

[11] Q. Zhang, F. Cao, W. Liu, K. Lukas, B. Yu, S. Chen, C. Opeil, D. Broido, G. Chen, and Z. Ren, "Heavy doping and band engineering by potassium to improve the thermoelectric figure of merit in p-type PbTe, PbSe, and $PbTe_{1-y}Se_y$," J. Am. Chem. Soc. **134**, 10031–10038 (2012).

[12] G. S. Nolas, M. Kaeser, R. T. Littleton, and T. M. Tritt, "High figure of merit in partially filled ytterbium skutterudite materials," Appl. Phys. Lett. **77**, 1855–1857 (2000).

[13] X. Shi, J. Yang, J. R. Salvador, M. Chi, J. Y. Cho, H. Wang, S. Bai, J. Yang, W. Zhang, and L. Chen, "Multiple-filled skutterudites: High thermoelectric figure of merit through separately optimizing electrical and thermal transports," J. Am. Chem. Soc. **133**, 7837–7846 (2011).

[14] R. J. LaBotz, D. R. Mason, and D. F. O'Kane, "The thermoelectric properties of mixed crystals of $Mg_2Ge_xSi_{1-x}$," J. Electrochem. Soc. **110**, 127–134 (1963).

[15] Y. Noda, H. Kon, Y. Furukawa, I. A. Nishida, and K. Masumoto, "Temperature dependence of thermoelectric properties of $Mg_2Si_{0.6}Ge_{0.4}$," Materials Transactions, JIM **33**, 851–855 (1992).

[16] V. K. Zaitsev, M. I. Fedorov, E. A. Gurieva, I. S. Eremin, P. P. Konstantinov, A. Y. Samunin, and M. V. Vedernikov, "Highly effective $Mg_2Si_{1-x}Sn_x$ thermoelectrics," Phys. Rev. B **74**, 045207 (2006).

[17] X. J. Tan, W. Liu, H. J. Liu, J. Shi, X. F. Tang, and C. Uher, "Multiscale calculations of thermoelectric properties of n-type $Mg_2Si_{1-x}Sn_x$ solid solutions," Phys. Rev. B **85**, 205212 (2012).

[18] J. J. Pulikkotil, D. J. Singh, S. Auluck, M. Saravanan, D. K. Misra, A. Dhar, and R. C. Budhani, "Doping and temperature dependence of thermoelectric properties in Mg_2(Si,Sn)," Phys. Rev. B **86**, 155204 (2012).

[19] H. Ihou-Mouko, C. Mercier, J. Tobola, G. Pont, and

H. Scherrer, "Thermoelectric properties and electronic structure of p-type Mg_2Si and $Mg_2Si_{0.6}Ge_{0.4}$ compounds doped with Ga," J. Alloys Compd. **509**, 6503 – 6508 (2011).

[20] W. Luo, M. Yang, F. Chen, Q. Shen, H. Jiang, and L. Zhang, "Fabrication and thermoelectric properties of $Mg_2Si_{1x}Sn_x$ ($0 \leqslant x \leqslant 1.0$) solid solutions by solid state reaction and spark plasma sintering," Materials Science and Engineering: B **157**, 96 – 100 (2009).

[21] W. Liu, X. Tang, and J. Sharp, "Low-temperature solid state reaction synthesis and thermoelectric properties of high-performance and low-cost Sb-doped $Mg_2Si_{0.6}Sn_{0.4}$," J. Phys. D: Appl. Phys. **43**, 085406 (2010).

[22] K. Mars, H. Ihou-Mouko, G. Pont, J. Tobola, and H. Scherrer, "Thermoelectric properties and electronic structure of Bi- and Ag-doped $Mg_2Si_{1x}Ge_x$ compounds," J. Electron. Mater. **38**, 1360–1364 (2009).

[23] V. Zaitsev, M. Fedorov, E. Gurieva, I. Eremin, P. Konstantinov, A. Samunin, and M. Vedernikov, "Thermoelectrics of n-type with ZT ¿ 1 based on Mg_2Si-Mg_2Sn solid solutions," in *Thermoelectrics, 2005. ICT 2005. 24th International Conference on* (2005) pp. 204–210.

[24] Y. Isoda, T. Nagai, H. Fujiu, Y. Imai, and Y. Shinohara, "The effect of Bi doping on thermoelectric properties of $Mg_2Si_{0.5}Sn_{0.5}$," in *Thermoelectrics, 2007. ICT 2007. 26th International Conference on* (2007) pp. 251–255.

[25] M. I. Fedorov, V. K. Zaitsev, and G. N. Isachenko, "High effective thermoelectrics based on the Mg_2Si-Mg_2Sn solid solution," in *Solid State Phenomena*, Vol. 170 (Trans Tech Publ, 2011) pp. 286–292.

[26] W. Liu, X. Tan, K. Yin, H. Liu, X. Tang, J. Shi, Q. Zhang, and C. Uher, "Convergence of conduction bands as a means of enhancing thermoelectric performance of n-type $Mg_2Si_{1-x}Sn_x$ solid solutions," Phys. Rev. Lett. **108**, 166601 (2012).

[27] M. B. A. Bashir, S. M. Said, M. F. M. Sabri, D. A. Shnawah, and M. H. Elsheikh, "Recent advances on $Mg_2Si_{1-x}Sn_x$ materials for thermoelectric generation," Renewable and Sustainable Energy Reviews **37**, 569 – 584 (2014).

[28] G. Jiang, L. Chen, J. He, H. Gao, Z. Du, X. Zhao, T. M. Tritt, and T. Zhu, "Improving p-type thermoelectric performance of Mg_2(Ge,Sn) compounds via solid solution and ag doping," Intermetallics **32**, 312 – 317 (2013).

[29] W. Liu, H. S. Kim, S. Chen, Q. Jie, B. Lv, M. Yao, Z. Ren, C. P. Opeil, S. Wilson, C.-W. Chu, and Z. Ren, "n-type thermoelectric material $Mg_2Sn_{0.75}Ge_{0.25}$ for high power generation," Proc. Nat. Acad. Sci. (USA) **112**, 3269–3274 (2015).

[30] K. Kutorasiński, J. Tobola, and S. Kaprzyk, "Calculating electron transport coefficients of disordered alloys using the KKR-CPA method and boltzmann approach: Application to $Mg_2Si_{1-x}Sn_x$ thermoelectrics," Phys. Rev. B **87**, 195205 (2013).

[31] K. Kutorasiński, B. Wiendlocha, J. Tobola, and S. Kaprzyk, "Importance of relativistic effects in electronic structure and thermopower calculations for Mg_2Si, Mg_2Ge, and Mg_2Sn," Phys. Rev. B **89**, 115205 (2014).

[32] W. Liu, K. Yin, X. Su, H. Li, Y. Yan, X. Tang, and C. Uher, "Enhanced hole concentration through Ga doping and excess of Mg and thermoelectric properties of p-type $Mg_{2(1+z)}(Si_{0.3}Sn_{0.7})_{1-y}Ga_y$," Intermetallics **32**, 352 – 361 (2013).

[33] D. Parker and D. J. Singh, "High-temperature thermoelectric performance of heavily doped PbSe," Phys. Rev. B **82**, 035204 (2010).

[34] H. Wang, Y. Pei, A. D. LaLonde, and G. J. Snyder, "Heavily doped p-type PbSe with high thermoelectric performance: An alternative for pbte," Adv. Mater. **23**, 1366–1370 (2011).

[35] G. Madsen and D. J. Singh, "Boltztrap. a code for calculating band-structure dependent quantities," Computer Phys. Commun. **175**, 67–71 (2006).

[36] D. J. Singh, "Electronic and thermoelectric properties of $CuCoO_2$: Density functional calculations," Phys. Rev. B **76**, 085110 (2007).

[37] D. Parker and D. J. Singh, "Potential thermoelectric performance from optimization of hole-doped Bi_2Se_3," Phys. Rev. X **1**, 021005 (2011).

[38] D. Parker and D. J. Singh, "High-temperature thermoelectric performance of heavily doped PbSe," Phys. Rev. B **82**, 035204 (2010).

[39] L. Zhang and D. J. Singh, "Electronic structure and thermoelectric properties of layered PbSe-WSe_2 materials," Phys. Rev. B **80**, 075117 (2009).

[40] D. J. Singh and L. Nordstrom, *Planewaves, Pseudopotentials and the LAPW Method, 2nd Edition* (Springer, Berlin, 2006).

[41] K. Schwarz, P. Blaha, and G. Madsen, "Electronic structure calculations of solids using the WIEN2k package for material sciences," Computer Phys. Commun. **147**, 71–76 (2002).

[42] J. P. Perdew, K. Burke, and M. Ernzerhof, "Generalized gradient approximation made simple," Phys. Rev. Lett. **77**, 3865–3868 (1996).

[43] F. Tran and P. Blaha, "Accurate band gaps of semiconductors and insulators with a semilocal exchange-correlation potential," Phys. Rev. Lett. **102** (2009).

[44] D. J. Singh, "Electronic structure calculations with the Tran-Blaha modified Becke-Johnson density functional," Phys. Rev. B **82**, 205102 (2010).

[45] J. Sun, H. Shi, M.-H. Du, T. Siegrist, and D. J. Singh, "Ba_2TeO as an optoelectronic material: First-principles study," J. Appl. Phys. **117**, 195705 (2015).

[46] V. Zaitsev, M. Fedorov, I. Eremin, and E. Gurieva, *Thermoelectrics Handbook: Macro to Nano* (CRC Press, 2005).

[47] J. Bourgeois, J. Tobola, B. Wiendlocha, L. Chaput, P. Zwolenski, D. Berthebaud, F. Gascoin, Q. Recour, and H. Scherrer, "Study of electron, phonon and crystal stability versus thermoelectric properties in Mg_2X(X = Si, Sn) compounds and their alloys," Func. Mater. Lett. **06**, 1340005 (2013).

[48] X. Liu, T. Zhu, H. Wang, L. Hu, H. Xie, G. Jiang, G. J. Snyder, and X. Zhao, "Low electron scattering potentials in high performance $Mg_2Si_{0.45}Sn_{0.55}$ based thermoelectric solid solutions with band convergence," Adv. Energy Mater. **3**, 1238–1244 (2013).

[49] Y. Pei, X. Shi, A. LaLonde, H. Wang, L. Chen, and G. J. Snyder, "Convergence of electronic bands for high performance bulk thermoelectrics," Nature **473**, 66–69 (2011).

[50] S. Bhattacharya and G. K. H. Madsen, "High-throughput exploration of alloying as design strategy for thermoelectrics," Phys. Rev. B **92**, 085205 (2015).

[51] X. Chen, D. Parker, and D. J. Singh, "Importance of nonparabolic band effects in the thermoelectric properties of semiconductors," Sci. Rep. **3**, 3168 (2013).

[52] N. A. Mecholsky, L. Resca, I. L. Pegg, and M. Fornari, "Theory of band warping and its effects on thermoelec-

tronic transport properties," Phys. Rev. B **89**, 155131 (2014).

[53] D. G. Cahill, S. K. Watson, and R. O. Pohl, "Lower limit to the thermal conductivity of disordered crystals," Phys. Rev. B **46**, 6131–6140 (1992).

[54] A. Khan, N. Vlachos, and T. Kyratsi, "High thermoelectric figure of merit of $Mg_2Si_{0.55}Sn_{0.4}Ge_{0.05}$ materials doped with Bi and Sb," Scripta Materialia **69**, 606 – 609 (2013).

[55] K. Kutorasiński, J. Tobola, S. Kaprzyk, A. Khan, and T. Kyratsi, "Electronic structure and thermoelectric properties of pseudoquaternary $Mg_2Si_{1-x-y}Sn_xGe_y$-based materials," J. Electron. Mater. **43**, 3831–3837 (2014).